SINTEF
PROCEEDINGS
1

Selected papers from 10th International Conference on Computational Fluid Dynamics in the Oil & Gas, Metallurgical and Process Industries

# Progress in Applied CFD

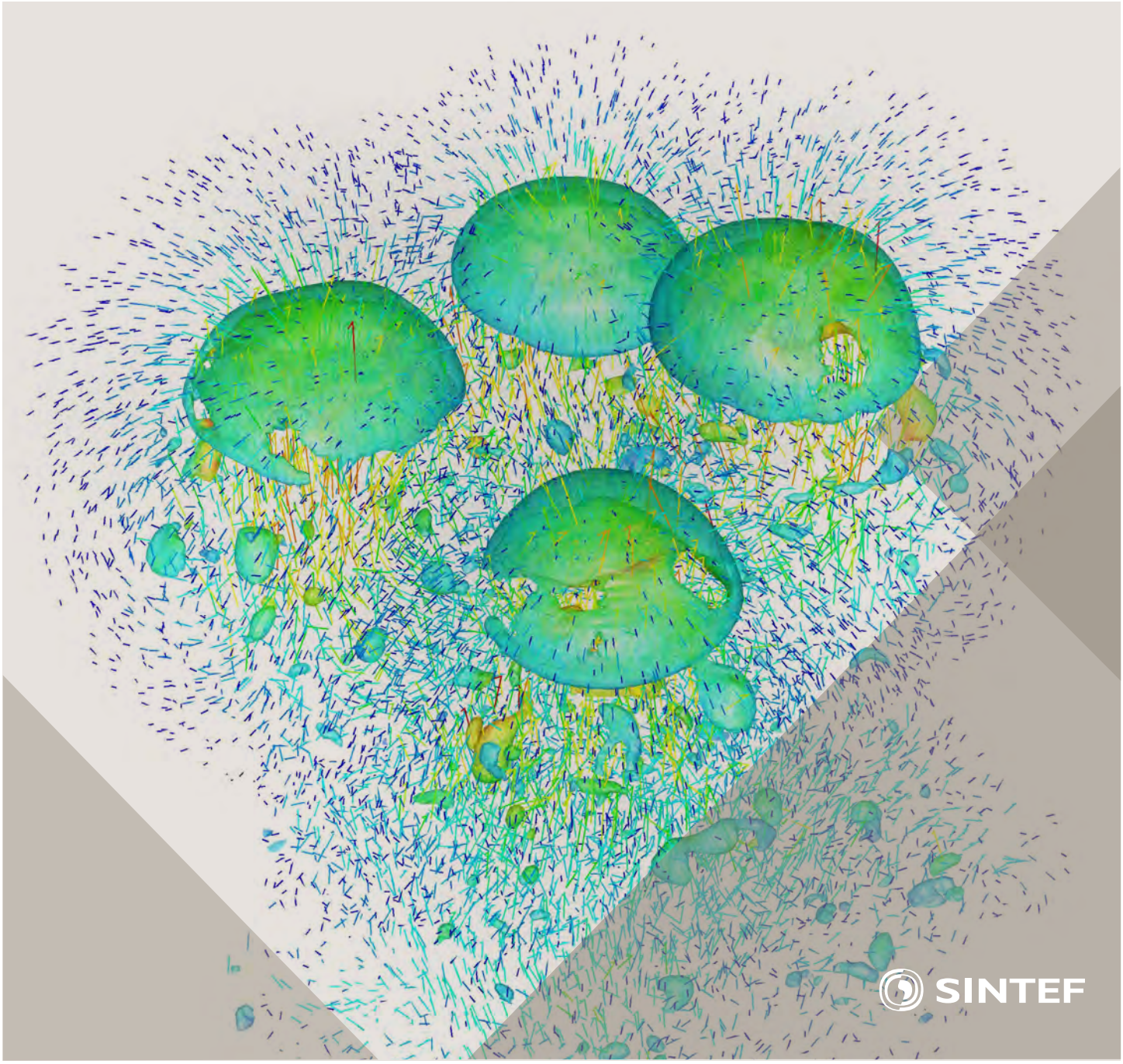

SINTEF Proceedings

Editors:
Jan Erik Olsen and Stein Tore Johansen

# Progress in Applied CFD

Selected papers from 10th International Conference on Computational Fluid Dynamics in the Oil & Gas, Metallurgical and Process Industries

SINTEF Academic Press

SINTEF Proceedings no 1
Editors: Jan Erik Olsen and Stein Tore Johansen
**Progress in Applied CFD**
Selected papers from 10th International Conference on Computational Fluid Dynamics in the Oil & Gas, Metallurgical and Process Industries

Key words:
CFD, Flow, Modelling

Cover, illustration: Rising bubbles by Schalk Cloete

ISSN 2387-4287 (printed)
ISSN 2387-4295 (online)
ISBN 978-82-536-1432-8 (printed)
ISBN 978-82-536-1433-5 (pdf)

60 copies printed by AIT AS e-dit
Content: 100 g munken polar
Cover: 240 g trucard



SINTEF Academic Press
Address: Forskningsveien 3 B
PO Box 124 Blindern
N-0314 OSLO
Tel: +47 22 96 55 55
Fax: +47 22 96 55 08

www.sintef.no/byggforsk
www.sintefbok.no

**SINTEF Proceedings**
SINTEF Proceedings is a serial publication for peer-reviewed conference proceedings on a variety of scientific topics.
The processes of peer-reviewing of papers published in SINTEF Proceedings are administered by the conference organizers and proceedings editors. Detailed procedures will vary according to custom and practice in each scientific community.

## PREFACE

This book contains selected papers from the 10th International Conference on Computational Fluid Dynamics in the Oil & Gas, Metallurgical and Process Industries. The conference was hosted by SINTEF in Trondheim in June 2014 and is also known as CFD2014 for short. The conference series was initiated by CSIRO and Phil Schwarz in 1997. So far the conference has been alternating between CSIRO in Melbourne and SINTEF in Trondheim. The conferences focus on the application of CFD in the oil and gas industries, metal production, mineral processing, power generation, chemicals and other process industries. The papers in the conference proceedings and this book demonstrate the current progress in applied CFD.

The conference papers undergo a review process involving two experts. Only papers accepted by the reviewers are presented in the conference proceedings. More than 100 papers were presented at the conference. Of these papers, 27 were chosen for this book and reviewed once more before being approved. These are well received papers fitting the scope of the book which has a slightly more focused scope than the conference. As many other good papers were presented at the conference, the interested reader is also encouraged to study the proceedings of the conference.

The organizing committee would like to thank everyone who has helped with paper review, those who promoted the conference and all authors who have submitted scientific contributions. We are also grateful for the support from the conference sponsors: FACE (the multiphase flow assurance centre), Total, ANSYS, CD-Adapco, Ascomp, Statoil and Elkem.

Stein Tore Johansen & Jan Erik Olsen

Organizing committee:

Conference chairman: Prof. Stein Tore Johansen
Conference coordinator: Dr. Jan Erik Olsen
Dr. Kristian Etienne Einarsrud
Dr. Shahriar Amini
Dr. Ernst Meese
Dr. Paal Skjetne
Dr. Martin Larsson
Dr. Peter Witt, CSIRO

Scientific committee:

J.A.M.Kuipers, TU Eindhoven
Olivier Simonin, IMFT/INP Toulouse
Akio Tomiyama, Kobe University
Sanjoy Banerjee, City College of New York
Phil Schwarz, CSIRO
Harald Laux, Osram
Josip Zoric, SINTEF
Jos Derksen, University of Aberdeen
Dieter Bothe, TU Darmstadt
Dmitry Eskin, Schlumberger
Djamel Lakehal, ASCOMP
Pär Jonsson, KTH
Ruben Shulkes, Statoil
Chris Thompson, Cranfield University
Jinghai Li, Chinese Academy of Science
Stefan Pirker, Johannes Kepler Univ.
Bernhard Müller, NTNU
Stein Tore Johansen, SINTEF
Markus Braun, ANSYS

## CONTENTS

10th International Conference on CFD in Oil & Gas, Metallurgical and Process Industries
SINTEF, Trondheim, Norway CFD 2014
17-19 June 2014

# MODELLING OF PARTICLE TRANSPORT AND BED-FORMATION IN PIPELINES

**C. Narayanan*, S. Gupta, D. Lakehal**

ASCOMP GmbH, Zurich, SWITZERLAND
*Corresponding author, E-mail address: chidu@ascomp.ch

**Keywords**: Two-phase flow, Eulerian-Lagrangian method, black powder, four-way coupling, VLES, LES

## ABSTRACT

Particle transport and bed formation in gas and condensate pipelines could occur under various flow regimes, from dilute flows to high mass-loading conditions, to conditions where particle beds form in the pipeline. Proper modelling requires a comprehensive approach that can handle all the different regimes. A range of complex phenomena have to be accounted for, including turbulence of the carrier phase, particle-turbulence and particle-wall interactions, surface roughness effects, particle-particle interactions, particle agglomeration, deposition, saltation and re-suspension. We present here recent results of TransAT's particle transport predictions to conditions of one-way, two-way and four-way particle-flow coupling, spanning the three flow regimes evoked: (i) dilute suspensions, (ii) high mass-loading conditions, and (iii) particle beds in the pipeline.

## INTRODUCTION

In dense particle-beds systems, the flow behaves in a very subtle way, with complex physical mechanisms taking place near the wall, where the particles accumulate. A number of simplified analytical solutions to determine the conditions of particle-bed removal in pipes and channels have indeed been proposed, but with limited success due to the simplifications implied. Today, intensive research is devoted to understand the conditions for dense particle-bed formation and removal, in hydrocarbon and in other related areas, but the difficulties encountered in measurements and flow visualization have hindered this progress.

In particle-laden pipelines, the particles tend to be transported through the pipeline by gas flow under specific conditions. The velocity required to move the particles could in some cases be estimated based on the pipeline diameter, gas pressure, and particle size and density (Tsochatzidis and Maroulis, 2007; Smart, 2007). Deposition of black powder will occur if there are solids in the pipeline fluid and the velocity is not high enough to drag the particles along by viscous flow forces. Sediment deposits can lead to blockage of the line, especially during pigging, while flowing powder can damage compressors, plug filters and damage user equipment. In extreme cases, the piping could be half full of black powder, causing shutdown of the compressor and up to 60 tons of black powder could subsequently be removed from the piping. Similarly, promising oil extraction techniques such as hydraulic fracturing involve transporting a proppant, such as sand, into rock fractures to keep them open and facilitate oil flow.

There are various incentives to explore the use of advanced prediction methods for this class of flows, featuring Lagrangian particle tracking spanning one to four-way particle-flow coupling, instead of average Euler-Euler formulations, Large Eddy Simulation (LES) instead of RANS, and transient rather than steady-state simulations. The current study which falls in this spirit presents a hierarchical modelling framework for the particle transport regimes mentioned above including validation and application of the model to select practical figures-of-merit (pressure drop in particle laden flows in pipes, and particle bed-formation and prediction of critical velocity of transport in pipes).

The modelling focuses on the statistical representation of particle-particle interactions close to the close-packing limit (collision stress) and particle-wall interactions, including the effect of statistical roughness. In terms of turbulence modelling, unsteady simulations will be used. Given the limitations of the RANS approach, LES and Very Large Eddy Simulation (VLES) methods will be emphasized, which have the ability to provide better flow unsteadiness needed to lift up the particles and move the deposited bed. The results were obtained with the CMFD code TransAT. The main issues and limitations will be discussed in the paper.

## THE PHYSICAL MODEL IN Trans*AT*

### The Numerical Approach

The CMFD code TransAT© (2014) is a multi-physics, finite-volume solver for the multi-fluid, Navier-Stokes equations. It uses structured multi-block meshes, and uses both the body-fitted coordinates (BFC) and immersed surface techniques (IST) for mesh generation. The solver is pressure based corrected for low-Mach number compressible flows. High-order schemes can be employed; up to $2^{nd}$-order schemes in space and $5^{th}$ order Runge-Kutta scheme in time. Multiphase flows with or without phase change can be tackled using interface tracking for both laminar and turbulent flows (Level Set and Phase Field), the phase averaged mixture model, and

the Lagrangian particle tracking, including with heat transfer.

### Turbulence Simulation (LES vs. VLES)

The basic idea of VLES (Johansen et al. 2004) is to combine RANS and LES for a specific flow, where the size of the most important scales can be identified. Here the flow is decomposed into a resolved and a subscale part, the latter being independent of the grid (in contrast to the sub-grid scale modelling in LES), but is dependent on the flow, and thus the flow characteristic length scale. Larger scales than this cut-off scale are resolved, while the rest are modelled, though with more refined statistical turbulence models than zero-equation ones, because turbulence sub-scales are neither isotropic nor independent of the boundary conditions, as speculated in LES. The approach assumes that the Kolmogorov equilibrium spectrum applies to the sub-filter.

### Lagrangian modelling for dilute systems

In this formulation, individual particles are tracked in a Lagrangian way within an Eulerian flow field. One-way coupling refers to the particle cloud not affecting the carrier phase, because the field is dilute. In contrast, two-way coupling refers to the scenario where the flow and turbulence are affected by the presence of particles (mildly charged but still in the dilute regime). In the one- and two-way coupling cases, the carrier phase is solved in the Eulerian way, i.e. solving for the continuity and momentum equations:

$$\nabla \cdot \boldsymbol{u} = 0 \tag{1}$$

$$\partial_t(\rho \boldsymbol{u}) + \nabla \cdot (\rho \boldsymbol{u}\boldsymbol{u}) - \nabla \cdot \boldsymbol{\tau} = -\nabla p + \boldsymbol{F}_b + \boldsymbol{F}_{fp} \tag{2}$$

This set of transport equations is then combined with the Lagrangian particle equation of motion:

$$d_t(v_{p_i}) = -f_d \frac{9\mu}{2\rho_p d_p^2}\left(u_{p_i} - u_i[x_p(t)]\right) \qquad f_d = 1 + 0.15 Re_p^{2/3} \tag{3}$$

where $\boldsymbol{u}$ is the velocity of the carrier phase, $\boldsymbol{u}_{p_i}$ is the velocity of the carrier phase at the particle location $\boldsymbol{x}_{p_i}$, $\boldsymbol{v}_{p_i}$ is the particle velocity, $\boldsymbol{\tau}$ is the viscous stress and $p$ the pressure. The source terms in Eq. (2) denote body force $\boldsymbol{F}_b$, and the rate of momentum exchange per volume between the fluid and particle phases, $\boldsymbol{F}_{fp}$. The coupling between the fluid and the particles is achieved by projecting the force acting on each particle onto the flow grid:

$$F_{fp} = \sum_{i=1}^{N_p} \frac{\rho_p V_p}{\rho_m V_m} R_{rc} f_i W(x_i, x_m) \tag{4}$$

where *i* stands for the particle index, $N_p$ for the total number of particles in the flow, $f_i$ for the force acting on a single particle centered at $\boldsymbol{x}_i$, $R_{rc}$ for the ratio between the actual number of particles in the flow and the number of computational particles, and $W$ for the projection weight of the force onto the grid node $\boldsymbol{x}_m$, which is calculated based on the distance of the particle from those nodes to which the particle force is attributed. $V_m$ is the fluid volume surrounding each grid node, and $V_p$ is the volume of a single particle (Narayanan and Lakehal, 2006).

### Lagrangian modelling for dense systems

The Eulerian-Lagrangian formulation for dense particle systems featuring mild-to-high volume fractions ($\alpha$ > 5%) in incompressible flow conditions is implemented in TransAT as follows (Eulerian mass and momentum conservation equations for the fluid phase and Lagrangian particle equation of motion):

$$\partial_t(\alpha_f \rho) + \nabla \cdot (\alpha_f \rho \boldsymbol{u}) = 0 \tag{5}$$

$$\partial_t(\alpha_f \rho \boldsymbol{u}) + \nabla \cdot (\alpha_f \rho \boldsymbol{u}\boldsymbol{u}) = -\nabla p + \nabla \cdot \boldsymbol{\tau} + \boldsymbol{F}_b + \boldsymbol{F}_{fp} - \boldsymbol{F}_{coll} \tag{6}$$

where $\alpha_f$ is the volume fraction of fluid ($\alpha_f + \alpha_p = 1$), $\boldsymbol{u}$ is the velocity of the carrier phase, $\boldsymbol{u}_{\mathrm{p}}$ is the velocity of the carrier phase at the particle location, $v_p$ is the particle velocity, $\Pi$ is the sum of viscous stress $\sigma$ and pressure $p$, $\tau$ is the turbulent stress tensor (depending whether RANS, V-LES or LES is employed).

In this dense particle context, the Lagrangian particle equation of motion (Eq. (3)) should have an additional source term $\boldsymbol{F}_{coll}$ denoting the inter-particle stress force. The inter-phase drag model in (Eq. (3)) is set according to Gidaspow (1986). The particle volume fraction is defined from the particle distribution function ($\phi$) as

$$\alpha_p = \iiint \phi V_p dV_p d\rho_p du_p \tag{7}$$

The inter-phase momentum transfer function per volume in the fluid momentum equation (Eq. (2)) is

$$F_p = \iiint \phi V_p [A] dV_p d\rho_p du_p; \tag{8}$$

with $A$ standing for the particle acceleration due to aerodynamic drag (1st term in the RHS of Eq. 3), i.e. excluding body forces and inter-particle stress forces (2nd and 3rd terms, respectively). The pressure gradient induced force perceived by the solids is not accounted for. The fluid-independent force $\boldsymbol{F}_{coll}$ is made dependent on the gradient of the so-called inter-particle stress, $\pi$, using

$$\boldsymbol{F}_{coll} = \nabla \pi / \rho_p \alpha_p \tag{9}$$

Collisions between particles are estimated by the isotropic part of the inter-particle stress (its off-diagonal elements are neglected.) In most of the models available in the literature $\pi$ is modelled as a continuum stress (Harris & Crighton, 1994), viz.

$$\boldsymbol{\pi} = \frac{P_s \alpha_p^{\beta(=2-5)}}{max[\alpha_{cp} - \alpha_p; \varepsilon(1-\alpha_p)]} \tag{10}$$

The constant $P_s$ has units of pressure, $\alpha_{cp}$ is the particle volume fraction at close packing, and the constant $\beta$ is set according to Auzerais *et al.* (1988). The original expression by Harris & Crighton (1994) was modified to remove the singularity at close pack by adding the expression in the denominator (Snider, 2001); $\varepsilon$ is a small number on the order of $10^{-7}$. Due to the sharp increase of the collision pressure, near close packing, the collision force (Eq. (9)) acts in a direction so as to push particles away from close packing. In practice the particle volume fraction can locally exceed the close packing limit marginally.

## ONE-WAY COUPLING: DROPLET DEPOSITION IN A PIPE

### Problem setup and modeling

The example discussed here was simulated using TransAT in the context of analyzing pipeline transport of natural gas and condensates. The objective is to predict the situation illustrated in Figure 1 (Brown et al., 2008), where liquid can be entrained under strong interfacial shearing conditions in the form of droplets from the liquid layer sitting at the bottom of the pipe. These should ultimately deposit on to the walls of the tube forming a film or redeposit back onto the pool itself. The core region consists of a mixture of gas and entrained liquid droplets. In the present study, it is assumed that entrainment of liquid droplets from the film on the upper surface of the pipe is negligible; an assumption consistent with experimental observations in relatively large diameter pipes (Brown et al., 2008).

A 3D body-fitted grid containing 500.000 cells well clustered near the pipe wall was generated. Two turbulence prediction strategies were employed: URANS and LES. The reason for this comparison is to identify the predictive performance of the models in reproducing the interaction between turbulence and the particles. The Lagrangian approach (1-3) under one-way conditions were employed to track the particles together with a particle-wall interaction model. The Langevin model for particle dispersion was used for RANS (Lakehal, 2002). In the LES, periodic boundary conditions along the pipe were employed to sustain turbulence; of course the pipe was shortened in length compared to RANS ($L = 2\pi D$).

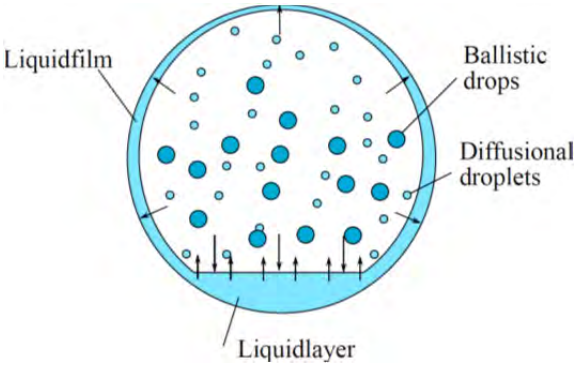


Figure 1: Schematic of the droplet entrainment model (extracted from Brown et al., 2008).

The WALE sub-grid scale model has been used for the unresolved flow scales only (not for particles). About 3000 droplets were injected, with a Gaussian size distribution around a 50 μm mean particle diameter, including: Range 1: $D_p$=1-48 μm; Range 2: $D_p$=49-85 μm ; Range 3: $D_p$=86-123 μm ; Range 4: $D_p$ =124-161 μm ; Range 5: $D_p$ =162-200 μm. Simulations were run on a 64 processor parallel cluster using the MPI protocol.

### Discussion of the results

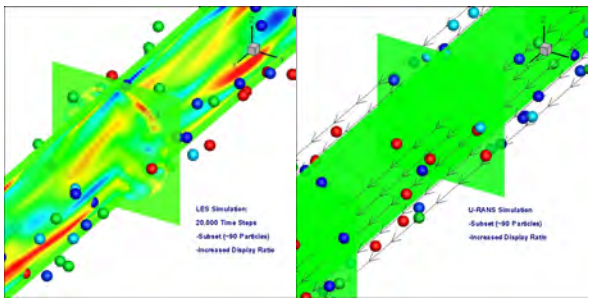

Figure 2: Snapshots of the flow in a gas pipe showing particle interaction with turbulence: left (LES); right (RANS).

The results depicted in Fig. 2 show a clear difference between URANS and LES. While the LES (left panel) depicts a clear turbulence dispersive effect on the particles, drifting some to the wall region, the URANS results (right panel) deliver a steady path of the particles with the mean flow. This is an important result, suggesting that albeit detailed 3D simulations, the results are sensitive to turbulence modeling.

The droplets population remaining in the gas core has been thoroughly studied by Lecoeur et al. (2013), and plotted as a function of two parameters (axial distance travelled in the pipe and the size of the droplets) for both RANS and LES. The results obtained show important discrepancies between the two approaches: (i) the droplet size has a more important effect in LES than in RANS: while in LES larger droplets tend to deposit faster than the smaller ones due to their ballistic nature (free-flight mechanism), in RANS, however, it seems that the smallest droplets do deposit faster than the large ones.

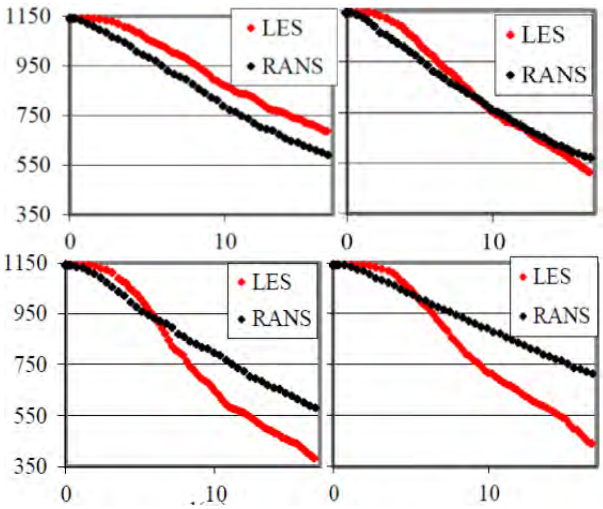


Figure 3: Cumulative number of droplets remaining in the pipe core for selected ranges of droplet sizes. (Upper panels) Range 1 ($D$=1-48 μm) and 2 ($D$=49-85 μm). (Lower panels): Range 3 ($D$=86-123 μm) and 5 ($D$=162-200 μm).

It was also found that the RANS-predicted deposition rate of droplets is rather monotone (see Fig. 4, black lines) and almost at equal rate or speed in the range 10-160 μm; differences start to be perceived for heavier droplets of diameter larger than 160 μm (see Fig. 3, black line in the 4th panel). The variation in the rate of droplet deposition is better depicted using LES, since particles of different sizes react differently to the various resolved eddies.

Looking closely at Figure 3 reveals more details about the rate of droplet deposition in the pipe. The number of droplets remaining in the gas core is shown there as a function of the axial distance travelled in the pipe, for all droplet-size ranges (10-48μm; 49-85μm; 86-123μm and 162-200μm). Smaller droplets (Range 1) tend to deposit faster in RANS than in LES; a tendency that changes gradually to Range 2 droplets that deposit equally be it with RANS or LES, to the extreme situation where ballistic droplets (Range 3 & 4) deposit much faster in LES than in RANS. Simply, LES is capable to distinguish between diffusional and free-flight deposition mechanisms (Botto et al., 2003).

## TWO-WAY COUPLING: HEAVY-LOADED PARTICULATE FLOW IN A PIPE

### Problem setup and modeling

The distribution of particles in a highly-loaded rough-wall channel was validated against experiments of Lain et al. (2002). The setup is a 2D channel of height 3.5cm and length 6m. The particles have a diameter of 130μm and a density of 2450 kg/m$^3$. The void fraction of the inflow fluid is set to a very small number (~0.001) so as to turn on the two-way coupling module. The mean inflow velocity was set to 20m/s in the x-direction with a standard deviation of 1.6m/s in x- and y-directions. The initial angular velocity of the particles was set to 1000 $s^{-1}$. A grid size of 125x34 was used. The simulations were run using the two-way coupling model and a Langevin forcing to account for the effects of turbulence on the particles. Further, since the pressure-drop in the channel is strongly affected by wall roughness, its effect on particles should be modelled, too. We use the model proposed by Sommerfeld and Huber (1999), which assumes that the particle impact angle is composed of the trajectory angle with respect to the wall and a stochastic component to account for wall roughness, $\alpha' = \alpha + \gamma\xi$, where $\xi$ is a Gaussian random variable with zero mean and a standard deviation of one, and $\gamma$ is a model constant. The particle wall restitution and friction coefficients are calculated using the expressions in Lain and Sommerfeld (2008).

### Discussion of the results

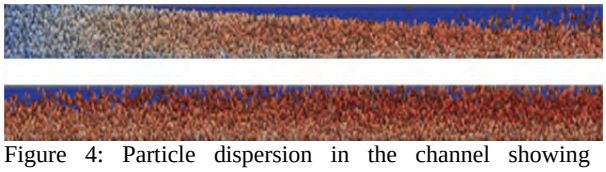

Figure 4: Particle dispersion in the channel showing re-suspension after a tendency for settling (two parts of the channel).

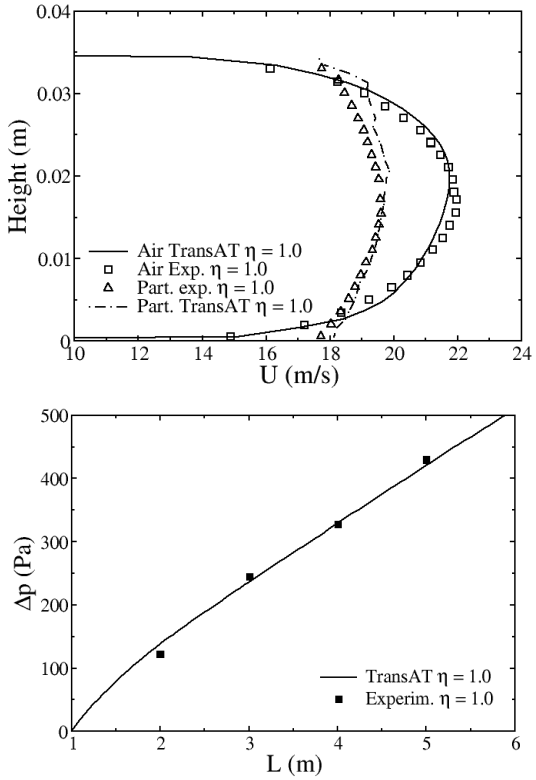


Figure 5: (upper panel) velocity profiles, and (lower panel) pressure drop in the pipe with wall roughness gradient of 1.5°, for a mass-loading of 1.0. : Exp. vs. TransAT

As seen in Fig. 4, as the simulation proceeds in time, a particle tends to move towards the bottom of the channel before re-suspension occurs thanks to the roughness model. The results in Fig. 5 (upper panel) show excellent agreement between the fluid and particle velocity profiles measured experimentally and those simulated by TransAT. The symmetry of the particle profile (like the fluid one) reflects the perfect dispersion of the particles in the channel, due to their systematic re-suspension caused by wall roughness. The lower panel of Fig. 5 shows that the simulation accurately predicts the pressure drop along the channel (the results are shown for a wall roughness gradient of 1.5 and a mass loading of 1).

## FOUR-WAY COUPLING

### Validation: Particle suspension sedimentation

This 3D problem was proposed by Snider (2001) as a case to validate his model. A well-mixed suspension of sand particles and air is left to settle to close pack solely due to the effect of gravity. The calculation parameters are given below. Particles are initially motionless and are uniformly, randomly distributed. The initial fluctuation in volume fraction is 0.3 on average as shown in Fig. 6. The heavy, large-size particles fall by the action of gravity in a 0.3m deep container filled with a lighter fluid (density ratio of 1/1000). The problem has an analytical solution to the evolution of the upper mixture interface between suspended particles and clarified fluid given by $h = gt^2/2$.

| | |
|---|---|
| Particle radius | 300 μm |
| Particle density | 2500 kg/m$^3$ |
| Fluid density | 1.093 kg/m$^3$ |
| Fluid viscosity | 1.95e-5 kg/ms |
| Initial particle volume fraction | 0.3 |
| Size of container | 13.8$^2$x30 cm$^3$ |
| Comp. Grid | 15x15x41 |

Table 1. Fluid flow conditions and parameters

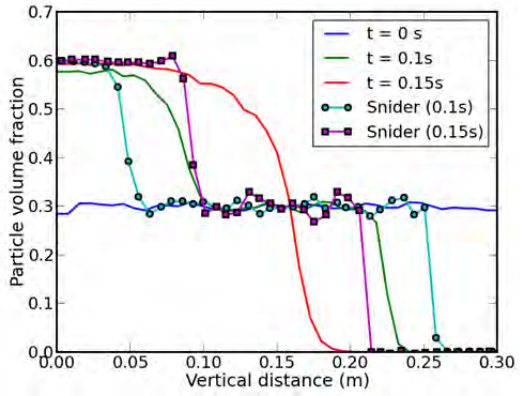


Figure 6: Volume fraction at times during sedimentation

Figure 6 shows the particle volume fractions, including comparison with the original data of Snider (2001). The interface between clarified fluid and mixture at 0.1s and 0.15s matches reasonably with Snider's (2001) data and with the analytical value of 0.25m and 0.19m from the bottom. Figure 7 shows that at 0.15s particles reach close packing at the bottom of the domain and at 0.2s no further settling has occurred. Figure 8 shows the particle distributions during settling at four instants (0.1, 0.15, 0.185 and 0.2s). The present four-way coupling solution, with the particle normal stress model as presented here and as implemented in TransAT, gives a natural settling to close pack.

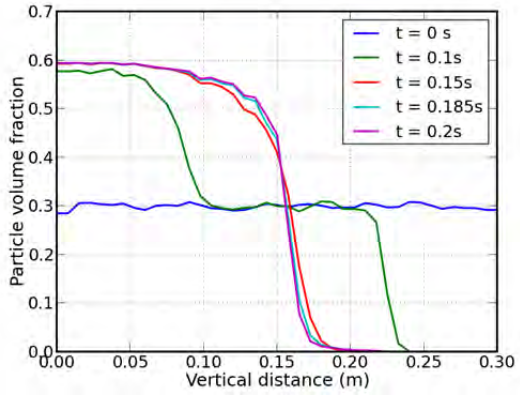


Figure 7: Volume fraction at times during sedimentation

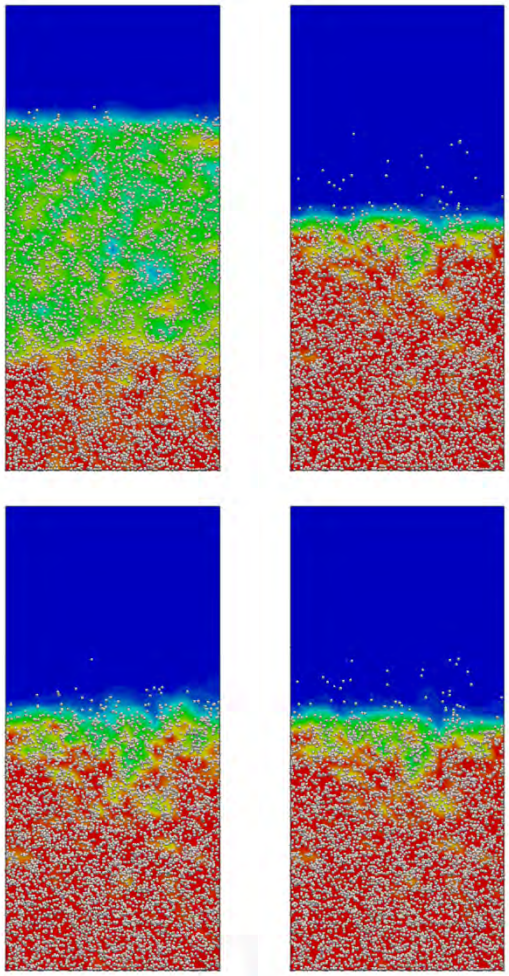

Figure 8: Particle volume-fraction distribution $\alpha_p$ (Red=0.6; Blue=0) at 0.1, 0.15, 0.185 and 0.2s.

## Sand-particle transport in a pipeline

Danielson (2007) proposes a model to predict the critical velocity of bed formation for particle transport in pipes, based on the assumption that there is a critical slip velocity between the sand and the fluid that remains constant over a wide range of flow velocities. Sand transported in (near) horizontal pipes will drop out of the carrier flow and form a stable, stationary bed at below critical velocities. The bed height develops to an extent such that the velocity of the fluid above the bed equals the critical velocity. When the velocity reaches a critical value, sand is transported in a thin layer along the top of the bed. A steady state is reached such that the sand eroded from the top of the bed is replaced by new sand from the upstream. At higher velocities, the sand bed breaks up into slow moving dunes and further increase in velocity results in sand transported as a moving bed at the bottom of the pipe. If the velocity is above the critical velocity, sand is entrained in the fluid flow:

$$U_c = \mathrm{K}\ \vartheta^{-1/9}\, d^{-1/9}\, [gD(s-1)]^{5/9} \qquad (11)$$

where K is a model constant equal to 0.23 based on SINTEF data (Danielson 2007) and $\vartheta$ is the fluid viscosity. The sand transport simulation is made here in two-dimensions with conditions given in Danielson (2007). Particles with diameter of 250, 350 and

450 μm are simulated for fluid velocities of 0.78, 1.2 and 1.6 m/s. The particle volume fraction at the inlet is 0.1. The channel length is 0.3m and height is 0.01 m, and is covered by 12 cells in the cross flow direction.

Figure 9 shows a set of results at four time instants; each set gathers results of the cases with fluid velocities of 0.78, 1.2 and 1.6 m/s, respectively. As the simulation proceeds in time a particle bed starts to form at the bottom of the channel and the inelastic wall reflection results in a non-homogeneous particle distribution along the height of the channel. There is a slowdown of fluid in regions of higher particle volume fractions at the bottom of the channel, and acceleration of the fluid in regions of lower particle volume fraction at the top of the channel. This is well captured due to the four-way coupling between particles and fluid momentum equations. The critical velocity predicted by Eq. (11) for a 3D pipe flow under these conditions is 4 m/s. For the simulation with inlet velocity of 0.78 m/s (first panel in each set), a stable bed is predicted with the fluid velocity at the top of the bed equilibrating to ~ 3m/s. Note that this is lower than the correlation most probably due to the fact that in the channel case, there is less wall friction (only at the bottom wall) than in a pipe. When the fluid velocity is increased (2$^{nd}$ and 3$^{rd}$ panels in each set), it can be seen in the images that the bed height indeed diminishes such that the flow velocity at the top of the bed is again approximately 3m/s. Further validation of the model for 3D pipes is necessary.

## Conclusions

The paper presents a simulation campaign of flows laden with solid particles of different size, under different flow conditions. Particle transport predictions were performed to conditions of one-way, two-way and four-way particle-flow coupling, spanning three flow regimes: (i) dilute suspensions, (ii) high mass-loading conditions, and (iii) suspension sedimentation and particle bed formation in pipelines.

## REFERENCES

F.M. Auzerais, R. Jackson, W.B. Russel, The resolution of shocks and the effects of compressible sediments in transient settling, *J. Fluid Mech*. 195, 437 (1988).

L. Botto, C. Narayanan, M. Fulgosi, D. Lakehal, Effect of near-wall turbulence enhancement on the mechanisms of particle deposition, *International Journal Of Multiphase Flow*, 31:8. 940 (2005).

L. Brown, G. Hewitt, B. Hu, C.P. Thomson, P. Verdin, Predictions of droplet distribution in low liquid loading, stratified flow in a large diameter pipeline, In Proc. BHR Conf. Cannes, France, May 2008.

T.J. Danielson, Sand transport in Multiphase pipelines, *OTC 18691*, Proc. Offshore Tech. Conf. Texas USA, 2007.

D. Gidaspow, Hydrodynamics of fluidization and heat transfer supercomputer modeling, *Appl. Mech. Rev.* 39, 1, (1986).

S.E. Harris, D.G. Crighton, Solutions, solitary waves and voidage disturbances in gas-fluidized beds, *J. Fluid Mech*. 266, 243 (1994).

S.T. Johansen, J. Wu, W. Shyy, 2004. Filtered-based unsteady RANS computations. *Int. Journal of Heat and Fluid Flow*, 25, 10-21, (2004).

S. Lain, M. Sommerfeld, J. Kissin, Experimental studies and modelling of four-way coupling in particle-laden horizontal channel flow, *Int. Journal of Heat and Fluid Flow*, 23, 647-656, (2002).

S. Lain, M. Sommerfeld, Euler/Lagrange computations of pneumatic conveying in a horizontal channel with different wall roughness, *Powder Technology*, 184, 76-88 (2008).

D. Lakehal, On the modelling of multiphase turbulent flows for environmental and hydrodynamic applications, International Journal of Multiphase Flow, 28:5. 823-863 (2002).

N. Lecoeur, C. Narayanan and G. Hewitt, The role of turbulence modeling in the simulation of droplet transport in annular flow, Proc. ICMF 2013, Jeju, Korea, 2013.

C. Narayanan, D. Lakehal, Particle transport and flow modification in planar temporally evolving laminar mixing layers. I.Particle transport under one-way coupling, *Physics of Fluids*, Part 1, 18: 9. 093302 (2006).

J. Smart, Determining the Velocity Required to Keep Solids Moving in Pipelines, *The Journal of Pipeline Engineering*, 6 No. 1 (2007).

D. M. Snider, An Incompressible Three-Dimensional Multiphase Particle-in-Cell Model for Dense Particle Flows, *JCP*, 170, 523–549, (2001).

M. Sommerfeld, N. Huber, Experimental analysis and modelling of particle–wall collision, *Int. J. Multiphase Flow, 25*, 1457–1489 (1999).

TransAT User Manual, (2010). www.ascomp.ch/transat.

N.A. Tsochatzidis, K.E. Maroulis, Methods help remove black powder from gas pipelines, *Oil & Gas Journal*, 03 (2007).

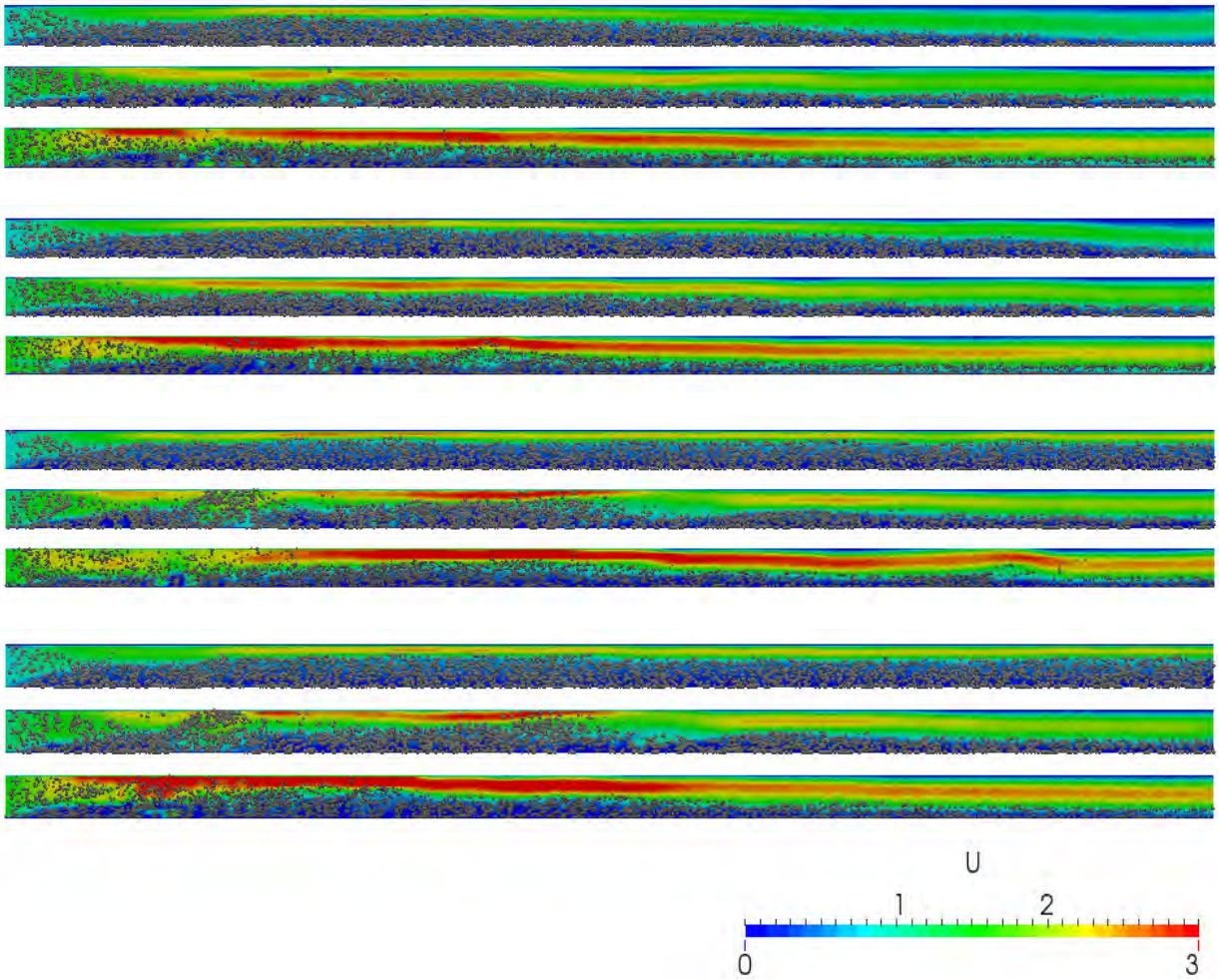


Figure 9: Particle distribution in the channel at 4 instants. Each set of panels refers to different inflow conditions (upper panel: 0.78m/s, middle panel: 1.2m/s, and lower panel: 1.6m/s). The last two time instants show the formation of a stable particle bed for the lowest inflow velocity case.